ACS APPLIED MATERIALS & INTERFACES

Research Article

www.acsami.org

Mechanism Studies on NanoPCR and Applications of Gold Nanoparticles in Genetic Analysis

Xinhui Lou* and Ying Zhang

Department of Chemistry, Capital Normal University, Beijing, 100048, China

Supporting Information

ABSTRACT: Recently, the applications of nanomaterial-assisted polymerase chain reaction (nanoPCR) have received considerable attention. Several potential mechanisms have been proposed, but mainly according to the results of PCR assays under specific conditions and lacking direct and general evidence. The mechanism of nanoPCR has not been elucidated yet. Here, taking gold nanoparticles (AuNPs) as an example, we report the three general effects of AuNPs: (1) AuNPs adsorb polymerase and modulate the amount of active polymerase in PCR, which was directly demonstrated by a simple and straightforward colorimetric assay and the dynamic light scattering measurements. (2) AuNPs adsorb primers and decrease the melting temperatures (T_m) of the duplexes formed with perfectly matched and mismatched primers and increase the T_m difference between them. (3) AuNPs adsorb PCR products and facilitate the dissociation of them in the denaturing step. All these effects were confirmed by addition of a rationally selected surface adsorbent, bovine thrombin, to highly efficiently modulate the surface adsorption of PCR components. These findings suggested that AuNPs should have multiple effects on PCR: (1) to regulate PCR in a case-by-case way via modulating the amount of active polymerase in PCR; (2) to improve PCR specificity in the annealing step via increasing the T_m difference between the perfectly matched and mismatched primers; (3) to improve PCR efficiency via speeding up the dissociation of the PCR products in the denaturing step. Taken together, we proposed the mechanism of nanoPCR is that the surface interaction of PCR components (polymerase, primers, and products) with AuNPs regulates nanoPCR. We further demonstrated that the applications of these findings improve the PCR of the amelogenin genes and Hepatitis B virus gene for genetic analysis. These findings could also provide helpful insight for the applications of other nanomaterials in nanoPCR.

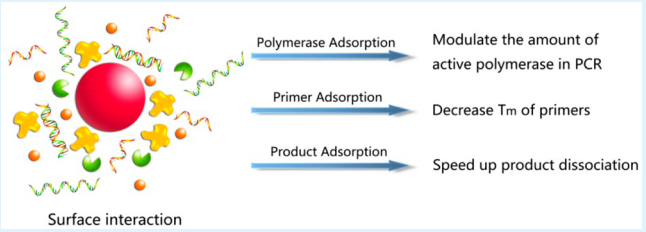

KEYWORDS: *polymerase chain reaction, gold nanoparticles, mechanism, nanoPCR*

1. INTRODUCTION

The polymerase chain reaction (PCR) has become one of the central techniques in molecular biology since its invention in the 1980s.[1,2] Despite its widespread applications, the technique is often fraught with difficulties. Over the years, great efforts have been made in both academia and industry to develop new reagents that can improve PCR efficiency and specificity. Well known PCR enhancers include small organic molecules (dimethyl sulfoxide,[3,4] glycerol,[5] betaine monohydrate,[4] formamide,[5,6] tetramethyl ammonium chloride, 7-deaza-2′-deoxyguanosine[7]), nonionic detergents (0.1−1% Triton X-100, Tween-20, or NP-40), and proteins (bovine serum albumin (BSA),[8,9] single stranded DNA binding protein (SSB)[9]).

Recently, a broad spectrum of nanomaterials including metal nanoparticles (NPs), metal oxide NPs, semiconductor quantum dots, carbon nanomaterials, silicon nanowires, and dendrimers has been applied in PCR to dramatically improve the specificity or sensitivity of PCR, referred to as nanomaterial-assisted PCR (nanoPCR).[10,11] For instance, Fan et al. reported the very first example of nanoPCR, in which gold nanoparticles (AuNPs) were able to improve the two-round PCR with respect to both the yield and specificity.[12] Pan and co-workers reported that, in the presence of an appropriate amount of AuNPs, they could obtain the target product even after six rounds of PCR.[13] Lin et al. reported that AuNPs increased the sensitivity of PCR detection 5- to 10-fold in a conventional PCR system and at least 10^4-fold in a quicker PCR system.[14] Later, Fan et al. reported an AuNP-based strategy to dynamically modulate the activity of DNA polymerases and achieve a hot start-like PCR with conventional Pfu polymerases.[15] With AuNPs assisted, the Pfu polymerase exhibited clearly hot start features. Very recently, AuNPs-PCR has been successfully coupled with capillary electrophoresis for high-throughput genotyping of long-range haplotypes to effectively discriminate DNA mismatches.[16] Along with these reports, several potential mechanisms for the effects of nanomaterials have been proposed. These include: (1) selective binding of single-stranded DNA (ssDNA) to nanomaterals in a manner analogous to ssDNA-binding protein (SSBs);[12,15,16] (2) the excellent heat transfer property of nanomaterials;[14] (3) adsorption of DNA polymerases with nanomaterials;[15,17] (4) condensation of PCR reactants on the surface of nanomateri-

Received: April 11, 2013
Accepted: June 4, 2013
Published: June 4, 2013

als;[18] (5) catalytic property of nanomaterials.[19] However, none of these mechanisms can well explain all the observed phenomena. These mechanisms were proposed mainly relying on the experimental observations of specific cases, and the direct and general evidence are required. Elucidation of a definite mechanism remains to be explored due to the complexity of PCR. It is thus necessary to make a systemic investigation to figure out the real mechanism of nanoPCR.

AuNPs are one of the most popular nanomaterials in the bioanalytical field due to their unique optical properties, good stability, biocompatibility, and simplicity in preparation and surface modification. The surface of AuNPs can adsorb the typical components (polymerase, DNA template, primers, and deoxyribonucleotide triphosphates (dNTPs)) in PCR with varied affinities and therefore is able to regulate PCR by modulating the concentrations of these components. In this work, taking AuNPs as an example, we found there were three general effects of AuNPs (Scheme 1): (1) AuNPs adsorb

Scheme 1. Schematics of the General Effects of Gold Nanoparticles (AuNPs) in PCR

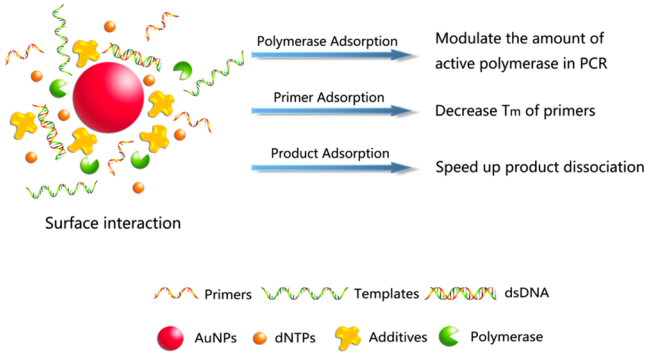

polymerase and modulate the amount of active polymerase in PCR, which is directly demonstrated by a simple and straightforward colorimetric assay and the dynamic light scattering measurements. (2) AuNPs adsorb primers and decrease the melting temperatures (T_m) of both complementary and mismatched primers and increased the T_m difference between them. (3) AuNPs adsorb PCR products and facilitated the dissociation of them in the denaturing step. All these effects were confirmed by addition of a rationally selected surface adsorbent, bovine thrombin, to modulate the surface adsorption of PCR components. These findings suggested that AuNPs should have multiple effects on PCR: (1) AuNPs modulate the amount of active polymerase in PCR and then regulate PCR. (2) AuNPs improve PCR specificity in the annealing step by increasing the T_m difference between the perfectly matched and mismatched primers. (3) AuNPs allows the efficient dissociation of the PCR products in the denaturing step.[14] We further demonstrated that these findings could facilitate the rational optimization of the PCR components and reaction conditions for genetic analysis. Taken together, these results suggest that AuNPs regulate PCR in multiple ways, which are all essentially controlled by the competitive adsorption of polymerase, primers, and products.

2. MATERIAL AND METHODS

2.1. Materials. PCR primers, mismatched primers, and the complementary strands were all synthesized by Sangon, Inc. (Shanghai, China) and purified by HPLC. The sequences were listed in Table 1, and the DNA stock solutions were all prepared with Rnase-free water. Human male genomic DNAs were purchased from Promega at the concentration of 172 μg/mL. QIAamp DNA Blood Mini kit was bought from Qiagen Inc. (Germany). Hepatitis B virus (HBV) serum samples were received from the hospital, and the typical gene sequences of the PCR targets were described in the Supporting Information. Bovine thrombin (TB), lysozyme from chicken egg white (Lys), y-globulins (y-Gl), and cytochrome c from equine heart (CC) were purchased from Sigma, and bovine serum albumin (BSA) was purchased from Invitrogen (CA, USA). Premix Taq Version 2.0 and SYBR Premix Ex Taq were all purchased from TaKaRa Bio. Co., Ltd. (Dalian, China) and used for regular PCR and real-time PCR (RT-PCR), respectively. SYBR gold nucleic acid gel stain was purchased from Invitrogen (CA, USA) for DNA staining in electrophoresis gel. Hydrogen tetrachloroaurate trihydrate ($HAuCl_4 \cdot 3H_2O$) and trisodium citrate were purchased from Acros Organics Inc. Colloidal AuNPs (13 nm) were prepared in our laboratory following the reported procedures.[20]

2.2. Colorimetric Competitive Adsorption Assay. Each sample contained deoxyribonucleotide triphosphates (dNTPs, 0.25 mM), forward primer GEN-FP (0.4 μM, Table 1), reverse primer GEN-RP (0.4 μM, Table 1), and BSA (1 μM)/TB (1 μM)/taqpolymerase (Taq, 1.5 U/100 μL) in 1× PCR buffer (10 mM Tris-HCl, pH 8.3, 50 mM KCl, 1.5 mM $MgCl_2$), followed by the addition of AuNP (final concentration of 1 nM). The photos were taken at 3 and 30 min, respectively.

2.3. Conventional PCR. PCR was performed using thermal cycler (Bio-Rad DNA Engine, Peltier Thermal cycler). For the PCR of the amelogenin gene, 50 μL of PCR mixture contained 25 μL of Premix Taq, male genomic DNA (172 ng), forward and reverse primers (GEN-FP and GEN-RP, 20 pmol, Table 1), and AuNPs (0−0.2 nM), with or without TB (or BSA) (0.01−2 μM). The binding specificities of the primers were confirmed using the BLAST program (http://www.ncbi.nlm.nih.gov/blast/). A typical PCR cycling condition consisted of an initial 30 s preheating at 95 °C, followed by 30−33 amplification cycles of denaturation at 94 °C for 30 s, annealing at 56 °C for 30 s, and extension at 72 °C for 30 s. Then PCR tubes were kept at 4 °C before gel electrophoresis. For the PCR of HBV, similar conditions were used with the addition of a certain amount of HBV serum sample or first-round PCR product as template. The specific conditions were listed in the figure caption (Figure 3). The DNA

Table 1. List of All Oligonucleotide Sequences Used in This Work

name	sequence (5′-3′)	description
GEN-FP	CACGAACTTTAATTAGTCACCTAC (24 bp)	forward primer for amelogenin genes
GEN-RP	TTAATTCCTCTCTCCATTATGTTC (24 bp)	reverse primer for amelogenin genes
ANTI-GEN-FP	GTAGGTGACTAATTAAAGTTCGTG (24 bp)	complementary to GEN-FP
ANTI-GEN-RP	GAACATAATGGAGAGAGGAATTAA (24 bp)	complementary to GEN-RP
GEN-FP-M1	CACGAACTTTAATTA**C**TCACCTAC (24 bp)	single-base mismatched forward primer
GEN-FP-M2	CACGAACTTTAATTA**C**T**G**ACCTAC (24 bp)	two-base mismatched forward primer
GEN-FP-M3	CACGAACTTTAATTA**C**T**G**A**G**CTAC (24 bp)	three-base mismatched forward primer
HBV-FP	TATGGGAGTGGGCCTCAGTC (20 bp)	forward primer for HBV
HBV-RP	CATCGTACTTTTCAATCAAT (20 bp)	reverse primer for HBV

extraction and sequence information of HBV serum sample was provided in the Supporting Information.

2.4. Fluorescence Measurement of Melting Temperature (T_m) of Primers. The T_m values were all measured using iQ 5 (Bio-Rad). Each 20 μL sample contains 10 μL of 2× SYBR Premix Ex Taq, forward primer (GEN-FP, GEN-FP-M1, GEN-FP-M2, or GEN-FP-M3) and ANTI-GEN-FP or reverse primer (GEN-RP) and ANTI-GEN-RP, followed by adding AuNP at 0.2, 0.5, or 1 nM, respectively. Set the program as: 95 °C 2 min, 75 °C 1 min, 55 °C 1 min, 35 °C 1 min, 25 °C 1 min, and 25 °C 30 s, to induce DNA hybridization; then, let the temperature rise from 25 to 85 °C and collect fluorescence data every 0.5 °C (with a 30 s dwell time) to get the melting curve.

2.5. Fluorescence Measurement of Dissociation Percentage of PCR Products. First, PCR was performed using iQ 5 (Bio-Rad). The 20 μL reaction mixtures contained 10 μL of 2× SYBR Premix Ex Taq, primers (GEN-FP and GEN-RP, 1 μM), and human male genomic DNA (344 ng), without or with TB (0.5 μM), respectively. AuNP (0.5 nM) was the last one added into the tubes. PCR cycling conditions consisted of an initial 30 s preheating at 95 °C, followed by 40 amplification cycles of denaturation at 95 °C for 30 s, annealing at 56 °C for 30 s, and extension at 72 °C for 30 s. Then, PCR tubes were maintained at 72 °C for 1 min. Second, the melting program was set as follows: the temperature rose at the max speed (3.3 °C/s) from 72 to 84 °C, and fluorescence data was colllected every 6 °C (with a 6 s dwell time, 72, 78, and 84 °C). All data was collected at the end of the 6 s dwell time.

2.6. Instrumentation. The hydrodynamic diameters of the particles were measure by Zetasizer Nano ZS90 (Malvern instruments Ltd., England) equipped with a red (633 nm) laser and an avalanche photodiode detector in particle size analysis mode. Three repeated measurements for each sample were conducted at 25 °C. PCR products were all analyzed by native polyacrylamide gel (PAGE) (10%), through a vertical electrophoresis system with the voltage set at 150 V, in 1× TBE buffer. After being stained with SYBR gold nucleic acid gel stain for 10 min, photos were taken through the gel documentation system (Bio-Rad Laboratories).

3. RESULTS

Most of the hypothesized mechanisms of nanoPCR were made according to the results of PCR assays under specific conditions and lacking direct and general evidence.[17] Here, we systemically study the general effects of AuNPs in PCR by directly monitoring and modulating the surface interactions (Scheme 1). For this study, we chosen the amelogenin genes (AMEL X and AMEL Y, Figure S-1, Supporting Information) as a model, which are present on both the X and the Y chromosomes and are routinely used for sex discrimination based on their size difference.[21,22] The gender determination method is based on a 90 bp deletion on the human X chromosome in an X−Y homologous region. According to the primer design (Table 1), the expected PCR products for a male sample consist of two products (79 and 169 bp) and for a female sample is a single product (79 bp).

3.1. AuNPs Adsorb Polymerase and Modulate the Amount of Active Polymerase in PCR. A typical PCR assay contains multiple components including dNTPs, primers, template DNA, double stranded DNA (dsDNA) products, and DNA polymerase, as well as some additives. In fact, it has been reported that dNTPs,[23,24] DNAs,[25−28] and proteins[29,30] were all able to nonspecifically adsorb onto the surface of citrate-coated AuNPs with varied affinities and kinetics. However, the adsorption of PCR components on AuNPs in a typical PCR mixture, which is critical for the mechanism study of nanoPCR, has not been reported yet.

The in situ observation and quantitative study of the competitive adsorption of multiple components on a surface is rather difficult. Here, taking advantages of the unique optical properties of AuNPs, the competitive adsorption of the PCR components can be directly visualized by the naked eyes and quantitatively measured by dynamic light scattering (DLS) measurements. As shown in Figure 1A, the AuNPs were

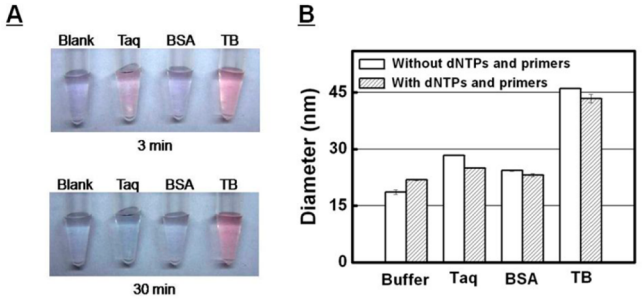

Figure 1. Competitive adsorption of dNTPs, primers, taqpolymerase, and additives on the surfaces of AuNPs in nanoPCR as demonstrated in the colorimetric assays (A) and by particle size measurements (B). Taq, BSA, and TB represent taqpolymerase, bovine serum albumin, and bovine thrombin, respectively. The samples for the size measurements were all prepared in 1× phosphate buffer (10 mM, pH 8.3) to avoid particle aggregation. The adsorbent concentrations were described in the experimental section.

respectively incubated with the PCR mixture (containing dNTPs (0.25 mM) and primers (GEN-FP, GEN-RP, Table 1, 0.4 μM) in the 1× PCR buffer) without and with Taq. Primers, dNTPs, and Taq were at the same concentrations as those in the PCR of the amelogenin genes performed in this work. After a 3 min incubation, the AuNPs colloid without Taq aggregated and turned blue. In contrast, the assay containing Taq remained dispersed and pink, which clearly demonstrated that Taq enhanced the stability of AuNPs.[14] The UV−vis measurements were also conducted to further demonstrate the increased stability in the presence of Taq (Figure S-2, Supporting Information). The DLS size measurements were subsequently conducted, and a dramatic increase in diameter was observed for the AuNPs incubated with Taq, suggesting Taq rapidly adsorbed onto AuNPs. Specifically, as shown in Figure 1B, the measured hydrodynamic diameter of the AuNPs in pure phosphate buffer (10 mM, pH 8.3) was 18.6 ± 0.6 nm, corresponding well with the size of AuNPs. At the presence of primers and dNTPs, the diameters increased to 21.9 ± 0.6 nm, due to the adsorption of primers and dNTPs. With the addition of Taq, the diameter of AuNPs was further increased to 25.0 ± 0.6 nm, indicating that Taq adsorbed onto the AuNPs even in the presence of high concentrations of primers and dNTPs.

Willson et al. have previously hypothesized the adsorption of polymerase on AuNPs, which was confirmed by using bovine serum albumin (BSA) as the competitive adsorbent to retrieve the PCR inhibition by an excess amount of AuNPs.[17] However, it is well-known that BSA itself can improve the efficiency of PCR. A high concentration of BSA in the PCR system could cause unknown effects on PCR, which would make the nanoPCR system more complicated. From this point of view, BSA is not an ideal PCR additive to modulate the adsorption of polymerase for the mechanism study. Inspired by their method, here we used a highly effective surface adsorbent, bovine thrombin (TB), at very low concentrations, to modulate the adsorption of Taq for the mechanism study to minimize the side effects caused by the adsorbent itself.

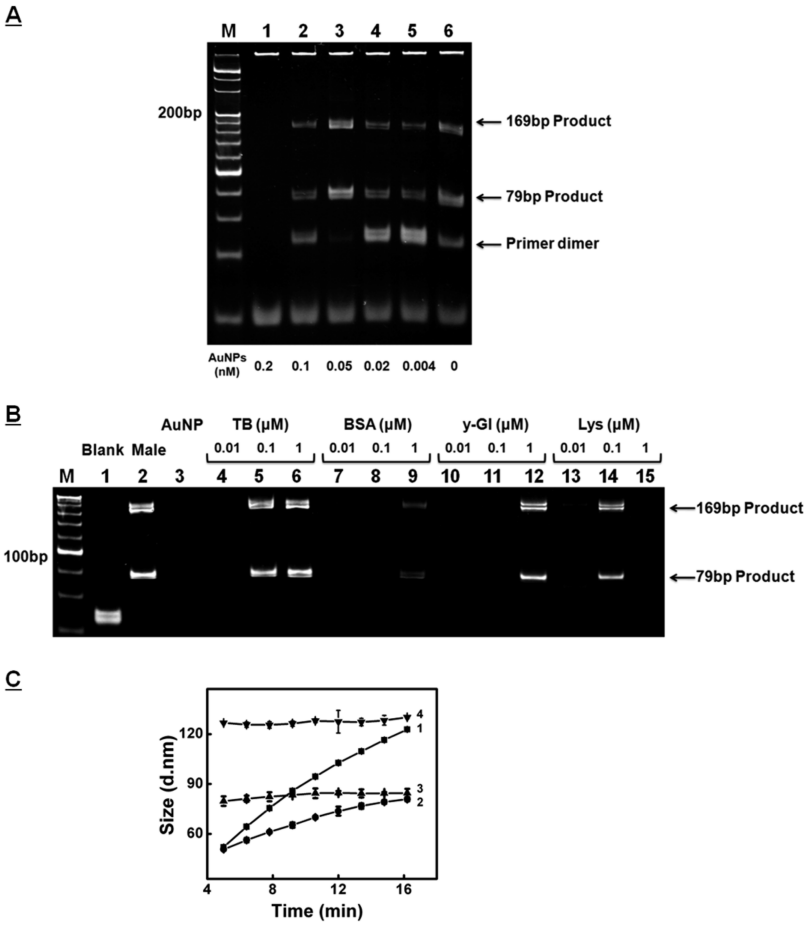

Figure 2. AuNPs regulated PCR via polymerase adsorption as demonstrated in (A) the effect of AuNPs on PCR of the amelogenin genes of a human male genomic sample; (B) the retrieval of PCR inhibition by bovine thrombin (TB), bovine serum albumin (BSA), y-globulins (y-Gl), and lysozyme (Lys); 20 bp marker (M); blank (lane 1); male genomic DNA sample (172 ng) without (lane 2) and with AuNPs (0.2 nM, lane 3); sample the same as the one in lane 3, but added in different concentrations of TB (lanes 4–6), BSA (lanes 7–9), y-Gl (lanes 10–12), and Lys (lanes 13–15); (C) the sizes of AuNPs with or without the presence of TB as a function of incubation time. Samples 1–4 contained 0, 0.01, 0.1, and 1 μM TB, respectively.

We proposed that a protein with higher pI value could be a more effective PCR additive based on the following fact. BSA has an isoelectric point (pI) of 4.7, which is significantly lower than the values of Taq (pI 6.0). The pH value of a typical PCR reaction mixture is around 8.3; thus, BSA would possess much more negative charges than Taq, resulting in the stronger electric repulsion with negatively charged DNAs and AuNPs and, therefore, less efficient adsorption on AuNPs. Exactly as we expected, BSA (1 μM) could not efficiently adsorb onto the surface of AuNPs, indicated by the blue color of the solution (Figure 1A) and the quite limited increase in particle size (4.5 nm, Figure 1B). The dimensions of BSA are 140 × 40 × 40 Å, and the formation of the monolayer of BSA would correspond to at least an 8 nm increase of the particle size. The results agree with the experimental facts that the high concentrations of BSA were required to fully retrieve the PCR inhibition caused by AuNPs by competing with Taq.[17]

TB is a biologically important, well-known serine protease protein that converts soluble fibrinogen into insoluble strands of fibrin, as well as catalyzing many other coagulation-related reactions.[31] Recently, with the discovery of the antithrombin aptamer,[32] thrombin has become the most popular used protein model in the aptamer selection methodology study[33−36] and in the development of protein detection technologies.[25,37,38] TB has a pI around 7, which is significantly higher than the values of BSA and Taq. TB at the same concentration of BSA was added into the AuNPs containing PCR buffer. As expected, the addition of TB significantly improved the stability of the AuNPs. As demonstrated in Figure 1A, after 30 min, only the AuNPs containing TB remained pink and all others turned blue due to aggregation, suggesting that TB was a highly effective surface adsorbent, much more effective than BSA. The dimensions of thrombin are 45 × 45 × 50 Å,[39] and the formation of the monolayer of thrombin would correspond to around a 9–10 nm increase of the particle size. The particle size dramatically increased to 43.4 ± 1.1 nm, suggesting multiple layers of TB adsorbed onto the surface of AuNPs. As shown above, TB is a highly efficient adsorbent for AuNPs compared to BSA.

In order to further confirm our claim that a protein with higher pI value could more effectively adsorb onto the surface of AuNPs, we tested other proteins with similar or higher pI values than TB (Figure S-3 and Table S-1, Supporting Information). Under the same condition as used in Figure 1A, similar to TB, the colloid remained pink after a 30 min incubation with 1 μM y-globulins (y-Gl, pI 6.85) or cytochrome c (CC, pI 10.0–10.5). The AuNPs partially aggregated in the presence of highly positively charged lysozyme (Lys, pI 11.35). In 1× PCR buffer, AuNPs incubated with y-Gl or CC remained pink and AuNPs incubated with Lys

dx.doi.org/10.1021/am4013209 | ACS Appl. Mater. Interfaces 2013, 5, 6276–6284

aggregated. The size measurements showed the significant increase of diameter of AuNPs in the presence of y-Gl or CC. When dNTPs and primers were in the mixture, the smaller diameters were observed due to the competitive adsorption with dNTPs and primers. Together, these data indeed verified that the proteins with a higher isoelectric point could more efficiently adsorb onto the surface of AuNPs.

We predicted that a more effective adsorbent should be able to modulate the adsorption of Taq and regulate PCR more efficiently. Taking the PCR of the amelogenin genes as an example, we first carried out the nanoPCR experiments with addition of AuNPs at varied concentrations (Figure 2A). The 0.05 nM AuNP was able to enhance PCR efficiency and specificity by increasing the PCR yield and minimizing the formation of primer dimer. In agreement with other reports,[12,17] the AuNP at higher concentrations (0.2 nM) completely inhibited the PCR. TB or BSA at varied concentrations was added into the AuNP (0.2 nM)-PCR assay. As the concentration of TB increased, more and more PCR products were formed and the PCR inhibition was completely retrieved when the concentration of TB reached 0.1 μM (Figure 2B, lane 5). In contrast, BSA at a 10 times higher concentration only retrieved around 12% of the PCR according to the intensity of the gel bands (Figure 2B, lane 9). The higher efficiency of TB to retrieve the PCR inhibition rather than BSA should be attributed to the higher efficiency of TB to be adsorbed onto AuNPs. Similar effects were also observed for y-Gl, Lys, and CC. Both Lys (Figure 2B) and CC (Figure S-4, Supporting Information) at very low concentration (0.1 μM) were also able to successfully retrieve the inhibition of PCR by AuNPs. The y-Gl protein was not as efficient as TB, Lys, and CC but still better than BSA (Figure 2B). Together, these data showed that the proteins with higher isoelectric point could more efficiently modulate the adsorption of Taq and regulate PCR more efficiently.

However, interestingly, the higher concentrations of CC/Lys (greater than 1 μM) could not retrieve the inhibition of PCR by AuNPs. We noticed a dramatic band intensity decrease in the upper well of the gel at the presence of 2 μM CC/Lys, indicating the significant loss of the template genetic DNA in the samples. The positively charged CC/Lys might electrically adsorb the negatively charged DNA template and then cause the failure of PCR. To confirm our hypothesis, we performed regular PCR without AuNPs but with Lys at varied concentrations. As shown in Figure S-5, Supporting Information, when the concentration of Lys was higher than 1 μM, the PCR was completely inhibited.

Considering that the surface adsorption of AuNPs was a kinetic process, we kinetically measured the sizes of AuNPs with or without the presence of TB (Figure 2C). We took the first measurements after a 5 min incubation with AuNPs. As we expected, the sizes of AuNPs in the presence of 0.1 and 1 μM TB were significantly greater than that of AuNPs in the absence of TB. The adsorption of TB at 0.1 and 1 μM was rapidly finished within 5 min, and the sizes of AuNPs were unchanged over the 18 min measurements, suggesting that TB was indeed highly efficiently adsorbed onto AuNPs in the PCR system. In contrast, the average sizes of AuNPs in the typical PCR mixture (Figure 2C, curve 1) without TB continuously increased over time. The increase of the sizes was attributed to the aggregation of AuNPs according to the UV−vis measurements, indicated by the decrease of the plasmon band at 520 nm and the increase of the adsorption around 600−700 nm (Figure S-6A, Supporting Information). The aggregation of the nanoparticles was partially and completely inhibited by the addition of 0.01, 0.1, and 1 μM TB, respectively, confirmed by the UV−vis measurements (Figure S-6, Supporting Information). After a 30 min incubation, the sample without and with 0.01 μM TB completely aggregated and turned blue, while the samples containing 0.1 and 1 μM TB stayed pink (Figure S-6E, Supporting Information). Interestingly, the PCR inhibition was completely retrieved when the TB concentrations reached a 0.1 μM or higher concentration due to the significantly decreased polymerase adsorption. The higher concentration of TB caused the formation of the thicker multiple layer of TB adsorbed onto the AuNPs. These results clearly indicated that polymerase adsorption plays an important role in regulating nanoPCR. The incubation time prior to PCR should also be an important factor to consider for the optimization of nanoPCR.

Please note that the particle sizes measured in this experiment were all much higher than those shown in Figure 1B, most possibly due to the significantly higher ionic strength of the PCR mixture than that of 1× PB, which significantly decreased the electrical repulsion between adsorbent and AuNPs and therefore resulted in the higher adsorption efficiency. To experimentally confirm this, we incubated AuNPs with 1 μM TB in three buffers with varied ionic strengths: 1/6 PCR buffer, 2/3 PCR buffer, and 1× PCR buffer, respectively (Table S-2, Supporting Information). The sizes of AuNPs significantly increased from 43.2 ± 0.4 to 56.0 ± 0.1 to 82.0 ± 2.5 nm as the total salt concentration (Tris-HCl, KCl, and $MgCl_2$) increased from 10 to 40 to 61.5 mM. In Figure 1, the ionic strength of the buffer (10 mM phosphate buffer) was similar to that of the 1/6 PCR buffer, and the AuNPs possessed almost the same size, 43.4 ± 1.1 nm. In Figure 2, Line 4, the buffer was 1× PCR buffer but also contained Taq and other ingredients from Premix Taq 2.0, which may make the size of AuNPs larger than in the pure 1× PCR buffer.

Above, we demonstrated that AuNPs can inhibit PCR in the presence of an excess amount of AuNPs by adsorbing polymerase. On the basis of the same mechanism, AuNPs should also be able to positively regulate PCR to improve the specificity or efficiency. For example, it is well documented that too much polymerase or template are the two possible reasons that cause the smear band and even completely inhibit PCR.[40] The excess amount of polymerase increases the likelihood of generating artifacts associated with the intrinsic 5′→3′ exonuclease activity of Taq, resulting in an excessive background of unwanted DNA fragments. Too much template DNA can cause the formation of the high percentage of the ssDNA products in the PCR mixture, showed as the smear band in the gel. Therefore, there is an optimized concentration for both polymerase and template for PCR. We confirmed the enhancement effect by conducting the second round of PCR of the HBV sample with varied initial template and polymerase concentrations. The first round PCR of the HBV sample was successful and clean with a single band formed at the expected position (Figure S-7, Supporting Information). The second round PCRs were then carried out by using different amounts of templates or polymerase. As shown in Figure 3A,B, too much template or polymerase all caused the formation of the smear band. The presence of AuNPs at 0.3 nM was able to improve the specificity of PCR for both situations (Figure 3C,D). The templates can adsorb onto the surface of AuNPs but less efficiently compared to polymerase, due to their highly negative charges and long length.[28] Therefore, the main contribution of

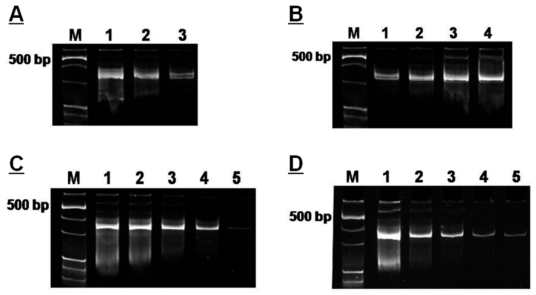

Figure 3. Second round of PCR of the HBV products from a 33 cycle amplification of the serum sample (Figure S-7, Supporting Information) under varied tempate (A), polymerase (B), and AuNP (C) concentrations. (A) Samples in lanes 1−3 contained 10, 100, and 1000 times diluted template from the first round of PCR and 0.375 U Taq in 15 μL. (B) Samples in lanes 1−4 contained 0.25, 0.5, 1, and 5 U Taq in 15 μL and 100 times diluted template from the first round of PCR. (C) Samples in lanes 1−5 contained 0, 0.1, 0.2, 0.3, and 0.4 nM AuNPs, and 10 times diluted template from the first round of PCR. (D) Samples in lanes 1−5 contained 0, 0.1, 0.2, 0.3, and 0.4 nM AuNPs and 1 U Taq in 15 μL.

AuNPs for the positive effect in PCR with an excess amount of polymerase or template should be the adsorption of the polymerase, rendering the optimization of the polymerase concentrations and the formation of the right products.

3.2. AuNPs Decrease the Melting Temperatures (T_m) of the Primers. According to the DLS measurements (Figure 1B), the diameters of AuNPs incubated with protein (BSA, Taq, and TB), primers, and dNTPs were all smaller than those of AuNPs incubated with protein only, indicating that the surfaces of AuNPs also have affinity with primers and dNTPs. Therefore, AuNPs might affect the T_m of primers and then the annealing temperatures required for PCR to maintain high specificity. We then tested the T_m values of the primers (GEN-FP, GEN-RP) with their perfectly complementary strands (ANTI-GEN-FP, ANTI-GEN-RP, Table 1) with or without the presence of AuNPs. The presence of 1 nM AuNPs caused 1.0 and 1.7 °C decreases of the T_m values of the forward and reversed primer with their perfect complementary strands, respectively (Figure 4A,B). Interestingly, the addition of 1 μM TB made the decreases of the T_m values significantly smaller (0.3 and 1.0 °C), which should be due to the decrease of the surface area of AuNPs available for the primer adsorption. Importantly, the decreases of T_m values of the primers with their mismatched complementary strands were greater than those with their matched strands at the same AuNP concentrations, resulting from the stronger interaction of ssDNA than dsDNA with AuNPs (Figure 4C, Figure S-8, Supporting Information).[25,28] The higher concentrations of the AuNPs were added, and the higher decreases in T_m values were achieved. The enlarged difference in T_m values between the primer with its perfectly matched and the mismatched stands would certainly favor the improvement in specificity. For example, the differences in T_m values between the strand (ANTI-GEN-FP) with its perfectly matched (GEN-FP) and one mismatched strand (GEN-FP-M1) with or without the presence of 1 nM AuNPs were 5.5 and 6.8 °C, respectively. At the same concentration of AuNPs, the higher the concentration of the primer, the more significant were the observed T_m decreases as shown in Figure 4, due to the stronger competition with other PCR components. For example, when the concentrations of GEN-FP and its complementary strand

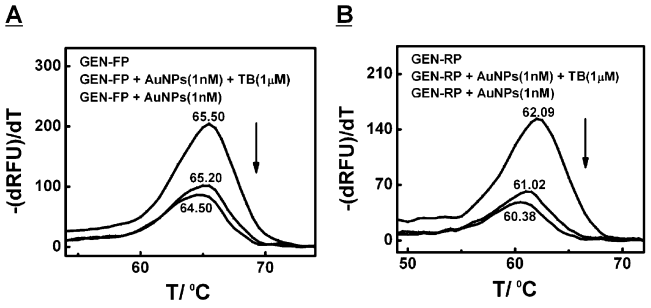

C

T / °C	GEN-FP	GEN-FP-M1	GEN-FP-M2	GEN-FP-M3
No AuNPs	66.4±0.1	60.9±0.1	55.6±0.1	53.3±0.2
Add AuNPs (0.2 nM)	66.2±0.1	60.6±0.1	55.4±0.1	53.1±0.1
ΔT	*0.2*	*0.3*	*0.2*	*0.2*
Add AuNPs (0.5 nM)	65.8±0.2	60.0±0.2	54.8±0.2	52.7±0.1
ΔT	*0.6*	*0.9*	*0.8*	*0.6*
Add AuNPs (1 nM)	65.0±0.1	58.2±0.5	53.3±0.3	51.5±0.1
ΔT	*1.4*	*2.7*	*2.3*	*1.8*

Figure 4. AuNPs decreased the T_m values of the forward (A), reversed (B), and mismatched primers (C). The concentrations of the oligonucleotides were 0.5 μM in (A) and (B) and 1 μM in (C), respectively. The error bars shown in (C) were calculated from five parallel experiments.

were 0.5 μM (Figure 4A) and 1 μM (Figure 4C), the T_m decreases in the presence of 1 nM AuNPs were 1.0 and 1.4 °C, respectively.

3.3. AuNPs Facilitate the Dissociation of the Products. We examined the effect of AuNPs on the dissociation percentage of the products by measuring the amount of dsDNA product as the function of heating temperature. The denaturing curves after PCR of the amelogenin genes of a human male sample were shown in Figure 5A. The two products (79 and 169 bp) had melting temperatures around 75 and 80 °C, respectively. The temperature of the mixture after PCR was raised from 72 to 84 °C at the maximum heating rate

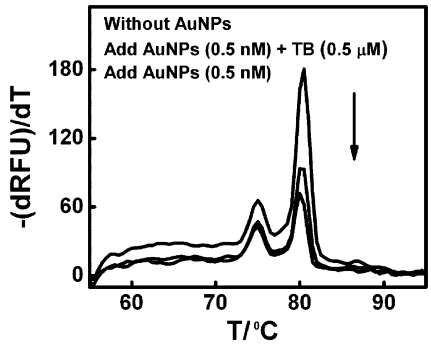

B

T (°C) \ DP[a]	Without AuNPs	Add AuNPs	Add AuNPs and TB
78 °C	42.4%±0.3%	47.9%±0.6%	44.5%±1.1%
84 °C	88.4%±0.7%	94.0%±0.9%	91.2%±1.7%

a: Represents the dissociation percentage of the PCR products.

Figure 5. AuNPs speed up the dissociation of the PCR products. (A) The denature curves of the PCR products of human male sample. (B) The dissociation percentages of the products at certain temperatures. The dissociation percentage defined as $(F_0 - F)/F_0$, where F_0 and F are the fluorescence intensities (RFU) at 72 °C and the set measuring temperatures (78 and 84 °C).

dx.doi.org/10.1021/am4013209 | ACS Appl. Mater. Interfaces 2013, 5, 6276−6284

of 3.3 °C/s, and the fluorescence measurements were conducted at 72, 78, and 84 °C (with a 6 s dwell time at each point), respectively. The double strand specific dye, SYBR-Green I, was used to quantitate the relative amount of double stranded PCR products in the PCR mixture. The dissociation percentage of the product was defined as $(F_0 - F)/F_0$, where F_0 and F are the fluorescence intensities (RFU) at 72 °C and the set measuring temperatures (78 and 84 °C). We found that the dissociation percentages of the PCR products at 78 °C without and with 0.5 nM AuNPs were 42.4 ± 0.3% and 47.9 ± 0.6%, respectively (Figure 5B). Interestingly, with the presence of both 0.5 nM AuNPs and 0.5 μM TB, the dissociation percentage of the PCR products at 78 °C was 44.5 ± 1.1%, greater than 42.4 ± 0.3% but smaller than 47.9 ± 0.6%. The data clearly showed that the surface interaction indeed enhanced the dissociation of the products and the dissociation efficiency can be regulated by the surface area of AuNPs available for product−AuNP interaction. A similar trend for dissociation percentage of the PCR product at 84 °C was observed. The dissociation percentages of the PCR products at 84 °C without, with 0.5 nM AuNPs, and with both AuNP and TB were 88.4 ± 0.7%, 94 ± 0.9%, and 91.2 ± 1.7%, respectively (Figure 5B).

4. DISCUSSION

4.1. AuNPs Can Regulate PCR in a Case-by-Case Way by Polymerase Adsorption. The polymerase adsorption mechanism has previously been proposed by several research groups to explain the observed phenomena in their individual studies.[15,17] They all agreed that AuNPs adsorb polymerase and caused a reduction in active polymerase concentration in PCR. They also agreed that AuNPs has a concentration-dependent effect on PCR. However, there is a disagreement on how AuNPs affect PCR by polymerase adsorption. For example, Willson et al. designed a semimultiplex PCR system with a forward primer and three reverse primers, containing two, one, and no mismatches, respectively. They found that the smaller amplicons were favored over the larger amplicons at elevated nanoparticle concentration, regardless of their specificity. According to this observation, they concluded that the effect of AuNPs was not to increase specificity but rather to favor smaller products over larger products by polymerase adsorption.[17] Nevertheless, Fan et al. has recently reported a gold-nanoparticle (AuNP)-based strategy to dynamically modulate the activity of DNA polymerases and realize a hot-start (HS)-like effect in the PCR, which effectively prevents unwanted nonspecific amplification and improves the performance of PCRs.[15] They hypothesized that the increased activity of polymerase at high temperatures was possibly due to the dissociation of Pfu from AuNPs at high temperature. In their study, they observed that AuNPs could inhibit not only long nonspecific products but also short ones. Similarly, in this work, we experimentally demonstrated that AuNPs can also minimize the formation of smaller amplicons, such as the primer−dimer (Figure 2A, lane 3), and the long and short smear bands (Figure 3C,D), especially, as we demonstrated that the surface adsorption of AuNPs strongly depends on the individual properties of proteins (Figure 1, 2B). Li et al. found that the AuNP-enhanced PCR efficiency largely depends on the type of polymerase.[14] Therefore, we believe that polymerase adsorption is indeed one of the main effects of AuNPs in nanoPCR. However, the final effect on PCR could be varied under specific PCR conditions and should be evaluated on a case-by-case basis.

4.2. AuNPs Can Improve the Specificity PCR by Primer Adsorption. For the first time, we experimentally demonstrated the AuNPs can adsorb primers by DLS measurements (Figure 1B), decrease the T_m of both complementary and mismatched primer double strands, and increase the T_m difference between them (Figure 4). There have been numerous reports on the differential binding abilities of AuNPs toward single stranded (ss) and double stranded (ds) DNA.[23,25,27,28,41] AuNPs bind to ssDNA much more strongly than dsDNA due to the exposure of the bases to Au. Thus, AuNPs can bind to the ssDNA regions of annealed primer duplex, preventing the rehybridization and decreasing T_m. On the basis of the close similarity between AuNPs and SSB, Fan et al. proposed an SSB-like mechanism for explaining AuNP-enhanced specificity of PCR.[12] Our results confirmed their hypothesized mechanism. Several degree increases in the difference of T_m values should not be the main factor contributing to the improved specificity at the extreme low annealing temperatures.[12] However, the bigger difference in T_m values between the primer with its perfectly matched and the mismatched stands would certainly favor the improvement in specificity. It should be a great advantage for the optimization of PCR conditions by selecting the appropriate annealing temperatures to dramatically improve the specificity of PCR. In addition, the examples we demonstrated in Figure 4 are not the optimized design, in which the mismatched primer−template (C/C) and complementary primer−template (G/C) were used. The affinity between AuNPs and four nucleotides is in the order: dAMP > dGMP ∼ dCMP > dTMP. Therefore, if the mismatched primer−template were A/C, a larger difference in T_m could be possible. Many other factors such as the mismatch position, primer length, and so on could also be optimized to further enlarge the difference in T_m. In fact, Fan et al. has recently reported the application of AuNPs for high-throughput genotyping of long-range haplotypes.[16] In their study, the mismatched primer−template (A/G) and complementary primer−template (A/T) were used and the clearly improved singlenucleotide polymorphism (SNP) detection was achieved. At the annealing temperature of 57 °C, the PCR with the single mismatched primer was completely inhibited by AuNPs. In contrast, in the absence of AuNPs, the PCR product yield with the complementary primers was only slightly higher than that using the mismatched primers.

4.3. AuNPs Can Improve PCR Efficiency by Product Adsorption. Liu et al. found that the PCR could be dramatically enhanced by AuNPs especially when the reaction time was shortened and the heating/cooling rates were increased.[14] They proposed that the excellent heat transfer property of AuNPs should be the major factor in improving the PCR efficiency. Agreeing with Willson,[17] we also doubt that the heat transfer property of AuNPs is the major contribution. In their report, the time spent for raising the temperature from 72 to 95 °C, maintaining at 95 °C, and decreasing to 72 °C was around 1 s/5 s/1 s and 13 s/5 s/13 s in the quicker and regular thermal cycler, respectively. The denaturing step in PCR allows the cycling of PCR. We suspect that the low efficiency or the failure of the PCR without AuNPs in the quicker thermal cycler was mainly due to the low denaturing efficiency of the products in such short time (7 s). The affinity of the products to the surface of AuNPs could speed up the dissociation rate of the products and then make the PCR successfully proceed in a

quicker thermal cycler. As demonstrated, we experimentally confirm our hypothesis that AuNPs indeed facilitate the dissociation of products due to the interaction between AuNPs and the products. We experimentally observed the increase of the dissociation efficiency of the PCR products in the presence of AuNPs. Such effect was attributed to the surface interaction between AuNPs and the products. Such affinity can facilitate the dissociation of PCR product and prevent its rehybridization in a manner similar to SSB. The SSB-like mechanism that Fan et al. proposed was used to explain the enhanced specificity of nanoPCR.[12] In this study, we for the first time experimentally demonstrated that the SSB-like mechanism also explains the enhanced PCR efficiency by AuNPs. It should be pointed out that the denature temperature in the typical PCR experiments is 95 °C, which is much higher than the temperatures used in our study. In our study, the lengths of the products were only 79 and 169 bp, which denatured much faster than the longer products under the same conditions. Therefore, the dissociation percentages were measured at lower temperatures to illustrate the enhancement effect of AuNPs for the dissociation of PCR products. It can be expected that AuNPs should also facilitate the dissociation of longer products. The longer products are usually more difficult than the shorter ones to denature. Therefore, the enhancement effect was more prominent for the amplification of longer products in Liu's study.[14]

These effects of AuNPs on PCR are essentially all based on the surface interaction with PCR components: polymerase, primers, and products. During PCR cycles, these components kinetically adsorb and dissociate from the surface of AuNPs.[15,19] Therefore, the final effect of AuNPs on PCR could be varied significantly from case to case, and careful optimization could be needed for specific applications.

5. CONCLUSION

In summary, we directly observed the three general effects of AuNPs in PCR: (1) AuNPs adsorbed polymerase; (2) AuNPs decreased the melting temperatures (T_m) of both complementary and mismatched primers and increased the T_m difference between them; (3) AuNPs facilitated the dissociation of the PCR products in the denaturing step. These observations suggested that AuNPs could regulate PCR in multiple ways, which are all essentially controlled by the competitive adsorption of polymerase, primers, and products. Specifically, AuNPs can both inhibit and enhance PCR by polymerase adsorption under varied situations. AuNPs can improve PCR specificity in the annealing step by increasing the T_m difference between the perfectly matched and mismatched primers. AuNPs allow the efficient dissociation of the PCR products in the denaturing step in the PCR cycle, contributing to the successful amplification in the shortened PCR time. Three general effects play together in PCR, and the main factor among them varies under different conditions. In addition, different types of nanomaterials have quite diverse surface properties. The findings reported in this work could provide helpful insight for the mechanism study and future applications of various types of nanomaterials in PCR.

■ ASSOCIATED CONTENT

Supporting Information

Additional information including the preparation of AuNPs and the HBV DNA sample, figures, and tables. This material is available free of charge via the Internet at http://pubs.acs.org.

■ AUTHOR INFORMATION

Corresponding Author

*E-mail: xinhuilou@cnu.edu.cn. Tel: +86-10-68902491 ext. 808. Fax: +86-10-68902320.

Notes

The authors declare no competing financial interest.

■ ACKNOWLEDGMENTS

We wish to thank Prof. Hongju Mao for providing the HBV clinical samples and Prof. Nengsheng Ye for providing y-Gl, CC, and Lys. This work was supported by National Natural Science Foundation (20975108), Beijing City Board of Education Science and Technology Program (KM201210028020), Program for the Young Talents of Higher Learning Institutions in Beijing (CIT&TCD201304145), Special Fund of State Key Joint Laboratory of Environment Simulation and Pollution Control (13K03ESPCT), the Scientific Research Foundation for the Returned Overseas Chinese Scholars, State Education Ministry, Beijing City Talent Training Aid Program (2012D005016000004), and National key scientific instrument and equipment development plan (2012YQ030111).

■ REFERENCES

(1) Saiki, R. K.; Gelfand, D. H.; Stoffel, S.; Scharf, S. J.; Higuchi, R.; Horn, G. T.; Mullis, K. B.; Erlich, H. A. *Science* **1988**, *239*, 487−491.

(2) Saiki, R. K.; Scharf, S.; Faloona, F.; Mullis, K. B.; Horn, G. T.; Erlich, H. A.; Arnheim, N. *Science* **1985**, *230*, 1350−1354.

(3) Shen, W. H.; Hohn, B. *Trends Genet.* **1992**, *8*, 227−227.

(4) Jensen, M. A.; Fukushima, M.; Davis, R. W. *PloS One* **2010**, *5*, No. e11024.

(5) Chakrabarti, R.; Schutt, C. E. *Nucleic Acids Res.* **2001**, *29*, 2377−2381.

(6) Sarkar, G.; Kapelner, S.; Sommer, S. S. *Nucleic Acids Res.* **1990**, *18*, 7465−7465.

(7) Musso, M.; Bocciardi, R.; Parodi, S.; Ravazzolo, R.; Ceccherini, I. *J. Mol. Diagn.* **2006**, *8*, 544−550.

(8) Nagai, M.; Yoshida, A.; Sato, N. *Biochem. Mol. Biol. Int.* **1998**, *44*, 157−163.

(9) Kreader, C. A. *Appl. Environ. Microbiol.* **1996**, *62*, 1102−1106.

(10) Pan, D.; Mi, L.; Huang, Q.; Hu, J.; Fan, C. *Integr. Biol.* **2012**, *4*, 1155−1163.

(11) Pan, D.; Wen, Y.; Mi, L.; Fan, C.; Hu, J. *Curr. Org. Chem.* **2011**, *15*, 486−497.

(12) Li, H. K.; Huang, J. H.; Lv, J. H.; An, H. J.; Zhang, X. D.; Zhang, Z. Z.; Fan, C. H.; Hu, J. *Angew. Chem., Int. Ed.* **2005**, *44*, 5100−5103.

(13) Pan, J.; Li, H.; Cao, X.; Huang, J.; Zhang, X.; Fan, C.; Hu, J. *J. Nanosci. Nanotechnol.* **2007**, *7*, 4428−4433.

(14) Li, M.; Lin, Y. C.; Wu, C. C.; Liu, H. S. *Nucleic Acids Res.* **2005**, *33*, No. e184.

(15) Mi, L.; Wen, Y.; Pan, D.; Wang, Y.; Fan, C.; Hu, J. *Small* **2009**, *5*, 2597−2600.

(16) Chen, P.; Pan, D.; Fan, C.; Chen, J.; Huang, K.; Wang, D.; Zhang, H.; Li, Y.; Feng, G.; Liang, P.; He, L.; Shi, Y. *Nat. Nanotechnol.* **2011**, *6*, 639−644.

(17) Vu, B. V.; Litvinov, D.; Willson, R. C. *Anal. Chem.* **2008**, *80*, 5462−5467.

(18) Cao, X.; Shi, X.; Yang, W.; Zhang, X.; Fan, C.; Hu, J. *Analyst* **2009**, *134*, 87−92.

(19) Cui, D. X.; Tian, F. R.; Kong, Y.; Titushikin, I.; Gao, H. J. *Nanotechnology* **2004**, *15*, 154−157.

(20) Lou, X. H.; Wang, C. Y.; He, L. *Biomacromolecules* **2007**, *8*, 1385−1390.

(21) Walker, J. A.; Hedges, D. J.; Perodeau, B. P.; Landry, K. E.; Stoilova, N.; Laborde, M. E.; Shewale, J.; Sinha, S. K.; Batzer, M. A. *Anal. Biochem.* **2005**, *337*, 89−97.

(22) Callinan, P. A.; Hedges, D. J.; Salem, A. H.; Xing, J.; Walker, J. A.; Garber, R. K.; Watkins, W. S.; Bamshad, M. J.; Jorde, L. B.; Batzer, M. A. *Gene* **2003**, *317*, 103−110.
(23) Lou, X. H.; Xiao, Y.; Wang, Y.; Mao, H. J.; Zhao, J. L. *ChemBioChem* **2009**, *10*, 1973−1977.
(24) Zhao, W.; Lee, T. M. H.; Leung, S. S. Y.; Hsing, I. M. *Langmuir* **2007**, *23*, 7143−7147.
(25) Zou, R.; Lou, X.; Ou, H.; Zhang, Y.; Wang, W.; Yuan, M.; Guan, M.; Luo, Z.; Liu, Y. *RSC Adv.* **2012**, *2*, 4636−4638.
(26) Liu, M.; Yuan, M.; Lou, X.; Mao, H.; Zheng, D.; Zou, R.; Zou, N.; Tang, X.; Zhao, J. *Biosens. Bioelectron.* **2011**, *26*, 4294−4300.
(27) Li, H. X.; Rothberg, L. J. *J. Am. Chem. Soc.* **2004**, *126*, 10958−10961.
(28) Li, H. X.; Rothberg, L. *Proc. Natl. Acad. Sci. U. S. A.* **2004**, *101*, 14036−14039.
(29) Lou, X. H.; He, L. *Sens. Actuators, B* **2008**, *129*, 225−230.
(30) Brewer, S. H.; Glomm, W. R.; Johnson, M. C.; Knag, M. K.; Franzen, S. *Langmuir* **2005**, *21*, 9303−9307.
(31) Hoppe, B.; Doerner, T. *Nat. Rev. Rheumatol.* **2012**, *8*, 738−746.
(32) Bock, L. C.; Griffin, L. C.; Latham, J. A.; Vermaas, E. H.; Toole, J. J. *Nature* **1992**, *355*, 564−566.
(33) Oh, S. S.; Plakos, K.; Lou, X.; Xiao, Y.; Soh, H. T. *Proc. Natl. Acad. Sci. U. S. A.* **2010**, *107*, 14053−14058.
(34) Lou, X. H.; Qian, J. R.; Xiao, Y.; Viel, L.; Gerdon, A. E.; Lagally, E. T.; Atzberger, P.; Tarasow, T. M.; Heeger, A. J.; Soh, H. T. *Proc. Natl. Acad. Sci. U. S. A.* **2009**, *106*, 2989−2994.
(35) Ahmad, K. M.; Oh, S. S.; Kim, S.; McClellen, F. M.; Xiao, Y.; Soh, H. T. *PloS One* **2011**, *6*, No. e27051.
(36) Miyachi, Y.; Shimizu, N.; Ogino, C.; Kondo, A. *Nucleic Acids Res.* **2010**, *38*, No. e21.
(37) Liu, J.; Cao, Z.; Lu, Y. *Chem. Rev.* **2009**, *109*, 1948−1998.
(38) Zheng, D.; Zou, R.; Lou, X. *Anal. Chem.* **2012**, *84*, 3554−3560.
(39) Bode, W.; Turk, D.; Karshikov, A. *Protein Sci.* **1992**, *1*, 426−471.
(40) Lorenz, T. C. *J. Vis. Exp.* **2012**, No. e3998.
(41) Wang, J.; Wang, L.; Liu, X.; Liang, Z.; Song, S.; Li, W.; Li, G.; Fan, C. *Adv. Mater.* **2007**, *19*, 3943−3946.